The Daily-Scale Entrance Dynamics of Intermittently Open/Closed Estuaries: Entrance Dynamics of Intermittently Open/Closed Estuaries

Article *in* Earth Surface Processes and Landforms · November 2017

DOI: 10.1002/esp.4280

CITATIONS
17

READS
484

3 authors, including:

Sarah Mcsweeney
University of Canterbury
29 PUBLICATIONS **269** CITATIONS

SEE PROFILE

Ian D Rutherfurd
University of Melbourne
145 PUBLICATIONS **4,126** CITATIONS

SEE PROFILE

The Daily-Scale Entrance Dynamics of Intermittently Open/Closed Estuaries

Sarah Louise McSweeney[1*], David M. Kennedy[1], Ian D Rutherfurd[1]

Corresponding Author Sarah Louise McSweeney

E-mail: sarah.mcsweeney@unimelb.edu.au

Address: University of Melbourne
School of Geography
221 Bouverie St
Parkville
Melbourne
Victoria
Australia
3010

DAVID M. KENNEDY

E-mail: davidmk@unimelb.edu.au

Address: The University of Melbourne
School of Geography
221 Bouverie St
Parkville
Victoria
Australia
3010

Ian D Rutherfurd

E-mail: idruth@unimelb.edu.au

Address: The University of Melbourne
School of Geography
221 Bouverie Street
Parkville
Victoria
Australia
3010

This article has been accepted for publication and undergone full peer review but has not been through the copyediting, typesetting, pagination and proofreading process which may lead to differences between this version and the Version of Record. Please cite this article as doi: 10.1002/esp.4280

Abstract

Intermittently Open/Closed Estuaries (IOCE) are a dynamic form of estuary characterised by periodic entrance closure to the ocean. Entrance closure is a function of the relative balance between on and offshore sediment transport with closures occurring during periods of low fluvial discharge whereby the estuary ebb-tidal prism is reduced. Although the broad scale processes of entrance closure are becoming better understood, there remains limited knowledge on channel morphodynamics during an individual closure event. In this study, the entrance dynamics of three IOCE on the coast of Victoria, Australia, are monitored over a daily timescale following both artificial and natural openings. The influence of changing marine and fluvial conditions on the relative sedimentation rate within the entrance channel is examined. IOCE in Victoria showed two distinct modes of entrance closure: (a) lateral accretion, whereby the estuary gradually closes by longshore drift-driven spit growth during low river flows, and (b) vertical accretion, where the channel rapidly aggrades under high (> 2 m), near-normal waves. During storms, when fluvial discharge and wave heights simultaneously increase, large swells will not always close the mouth due to an increase in the ebb-tidal prism. The estuary water depth and the maximum channel dimensions following opening were not proportional to the opening duration, with this being a function of the wave and fluvial conditions occurring following lagoon drainage. Based on the findings of this work, implementing a successful artificial entrance opening is dependent on reduced onshore sedimentation rates which occurred when wave energy is low (< 2 m Hs) relative to river flow.

Introduction

Intermittently Open/Closed Estuaries (IOCE) are systems characterised by periodic entrance closure. They are found on wave-dominated microtidal coasts and are located at the mouths of rivers with low or variable fluvial discharge (Cooper, 2001; Perissinotto et al., 2010). There are at least 1,477 IOCE globally, comprising approximately 15.30 % of all estuaries on wave-dominated microtidal coasts, and with 84 % of all IOCE occurring in temperate climates (McSweeney et al., 2017a). Internationally, IOCE are referred to by a range of terms including Intermittently Closed/Open Lakes and Lagoons (ICOLLs) (Roy et al., 2001), bar-built estuaries (Largier and Taljaard, 1991), and Temporarily Open/Closed Estuaries (TOCE) (Snow and Taljaard, 2007). Closure occurs when a subaerial berm forms in the entrance channel. Closure can occur both seasonally (e.g. Wilson Inlet, Western Australia: Neira and Potter, 1992; Ranasinghe and Pattiaratchi, 2003) or irregularly throughout the year (e.g. Anglesea River, southeast Australia: McKenzie et al., 2011). Entrance closure will then persist for days to years and is often associated with flooding and a deterioration in water quality of the enclosed lagoon (Jones and West, 2005; Gale et al., 2006; O'Neill et al., 2015).

Estuary entrance closure is a function of the relative balance between on and offshore sediment transport within the entrance channel (Fortunato et al., 2014; Garside et al., 2014; Hinwood and McLean, 2015) (Figure 1). Closure occurs during periods of low river flow when wave-driven onshore deposition surpasses the ability of ebb-tidal currents to remove sediment from the channel (Gao and Collins, 1994; Morris and Turner, 2010; Whitfield et al., 2012; Ranasinghe et al., 2013). Longshore drift and

cross-shore wave processes have been broadly identified as the main drivers of entrance closure (Ranasinghe and Pattiaratchi, 1999; 2003) (Figure 1). For example, when ebb-tidal velocity is high and interrupts longshore deposition, the estuary remains open and a subtidal shoal forms up-drift of the mouth, with a second smaller shoal sometimes forming down drift (FitzGerald, 1988; Ranasinghe et al., 1999). When ebb-tidal velocity decreases, these shoals migrate alongshore to close the entrance (Jarrett, 1976; Ranasinghe et al., 1999). Longshore drift as a driver of entrance closure is most common under an oblique angle of wave approach (Aubrey and Gaines, 1982; Nordstrom et al., 2003; Monge-Ganuzas et al., 2015) and on straight beaches with high longshore transport rates (Ranasinghe and Pattiaratchi, 2003). In situations characterised by cross-shore transport, entrance closure is related to onshore sediment transport under long-period swell conditions when ebb-tidal currents are weak (Ranasinghe and Pattiaratchi, 1999; 2003). Cross-shore closures are most common on embayed beaches (FitzGerald, 1988; Treloar et al., 1993; Cooper, 1994; Ranasinghe et al., 1999) and have only been described for IOCE which open and close on a regular seasonal basis (Ranasinghe and Pattiaratchi, 2003; Vu et al., 2014).

Individual storm events are critical agents of change on beach systems (Leatherman, 1979; Aleman et al., 2015). They also facilitate berm and channel deposition at the entrances of IOCE when large waves increase the rates of sediment transport by swash overtopping and longshore drift (Baldock et al., 2008; Hanslow et al., 2000; Morris and Turner, 2010; Slinger, 2016). Deposition rates within an estuary entrance during storms is dependent on: (1) the available accommodation space within the channel, (2) the spatial divergence in sediment transport (Wainwright et al., 2011), (3) nearshore wave conditions (Morris and Turner, 2010), (4) the directional and

frequency characteristics of the wave spectrum (Hanes et al., 2011), (5) fluvial inflow and ebb-tidal velocity (Bruun and Gerritsen, 1960; O'Brien and Dean, 1972; Ranasinghe et al., 2013), and (6) sediment availability. Although these broad scale drivers are becoming better understood, there is limited knowledge on channel morphological dynamics during an individual closure event, especially over an hourly to daily scale. A key question that remains is whether onshore sediment transport follows a uniform pathway of ingress into the entrance once the lagoon has drained, or if it varies over time based on the concurrent marine and fluvial conditions.

This study sets out to quantify the entrance dynamics of IOCE over an hourly to daily scale to examine the specific geomorphic processes that control entrance behaviour. A field-based approach is undertaken through quantifying entrance morphology prior to and throughout several entrance opening events at the Aire, Gellibrand, and Anglesea River estuaries (Victoria, Australia). These IOCE were selected to be representative of IOCE on microtidal, open sandy coastlines in temperate regions globally, being the boundary conditions where most IOCE are located (McSweeney et al., 2017a). The study aims to quantify the rate of change in channel morphology under different geomorphic conditions with a primary focus entrance closure processes. This is relevant as in practice the majority of IOCE are artificially opened before their natural opening threshold can be reached. Field data is used to (a) test if the known drivers of closure established for seasonally open estuaries are applicable to IOCE that close multiple times throughout the year; (b) identify what conditions promote rapid entrance closure; and (c) identify how different depositional processes are reflected in the change in channel morphology. Understanding how different marine and fluvial conditions control the rate of channel deposition will enable knowledge to be applied

in the context of initiating effective, long-lived artificial openings thus saving managers considerable time and money.

Regional setting

The open coast of western Victoria, Australia, is microtidal with mixed semidiurnal tides and a spring tidal range of 0.80 - 1.60 m. There is a prevailing southwesterly swell with >20 % of all breaking waves being >2 m (Hodgkin and Hesp, 1998). The mean annual significant wave height is 2.49 m and mean annual maximum wave height 4.13 m (Table 1). Peak wave heights occur during May to September and the mean annual wave period is 12.51 sec (Table 1). The mean annual offshore wave direction is 213°N (Table 1) which results in a dominant easterly longshore drift (Barton and Sherwood, 2004). During June - September, waves approach from the SW with a slight shift to the SSW occurring during summer (Table 1). In spring and summer, local winds from the southeast increase in frequency (Barton and Sherwood, 2004). This seasonal variability in local winds can also influence the longshore drift direction, with a westerly drift described to occur from summer to early autumn in some compartments of the coast (Barton and Sherwood, 2004; Pope, 2011). Victoria has a temperate climate with rainfall and river discharge being both seasonally and interannually variable (Risbey et al., 2009; Kennard et al., 2010). Rivers draining coastal catchments in Victoria experience peak flows in winter and spring, with low flows during summer (Puckridge et al., 1998). Rivers in the study region provide a negligible terrigenous sediment supply to the coast and coastal deposition is nourished primarily from shelf derived carbonates (Davis Jr, 1989; Nichol et al., 1994). This is due to the small size of most rivers (by both Australian and global standards) (Davis

Jr, 1989), the relatively low relief (Milliman and Syvitski 1992; Harris et al., 2002), and the potential for storage in the central basins of estuaries which act as a sink for sediment (Kench, 1999).

The study was conducted at three IOCE on the west Victorian coast: the Gellibrand, Aire and Anglesea River estuaries (Figure 2). The Gellibrand River (38.69°S, 143.16°E) is the largest of all sites with a catchment area of 1,184 km^2, length of 7.80 km, and spring tidal prism of 3.60 x 10^6 m^3. The Gellibrand has a mature upper estuary basin in the final stages of sedimentary infill with an alluvial floodplain >1 km wide (Tunbridge and Glenane, 1988; Roy et al., 2001). Upstream of the mouth, the channel reaches a maximum of 3 m depth with the catchment predominantly used for forestry (40 %) and agriculture (36 %) (Mondon et al., 2003). The mean daily discharge is 7.94 m^3/s and mean annual rainfall is 1,077 mm/year. The Gellibrand has a mean opening duration of 39 days and is artificially opened 1 - 2 times per year on average (Estuary Watch Victoria, 2017). During the study period, the Gellibrand River was artificially opened once (Table 2). The Aire River estuary (38.76°S, 143.51°E) is smaller than the Gellibrand with a catchment area of 250 km^2, length of 6.70 km, and spring tidal prism of 4.60 x 10^6 m^3. While exposed to direct SW swells propagating from the Southern Ocean, the 1 km long estuarine beach is bound by headlands on either side. The dominant catchment land uses are forestry (40 %), agriculture (24 %) and native forest (18 %) (Mondon et al., 2003). The mean daily discharge is 0.82 m^3/s and mean annual rainfall is 895 mm/year. The Aire River estuary is in the mid to late stages of sedimentary infill, with an extensive alluvial floodplain surrounding the backing lagoon. Aire River was opened three times artificially and once naturally throughout the study period (Table 2). The Anglesea River estuary (38.46°S, 144.90°E) has the smallest

dimensions of all sites with a catchment area of 125 km^2, length of 3.50 km, and spring tidal prism of 1.20 x 10^6 m^3. The catchment is moderately urbanized (5 %) and farmed (5 %) but is largely part of a coal mining lease (Mondon et al., 2003). Anglesea River has a constant mean daily discharge of 0.05 m^3/s maintained by the Alcoa Coal Plant (Sharley et al., 2012) and a mean annual rainfall of 635 mm/year. The mean opening duration is 14 days with the site artificially opened 2 - 3 times per year on average (Estuary Watch Victoria, 2017). Throughout the study period Anglesea River was opened once artificially (Table 2).

Methods

Entrance channel morphology was analysed using a Trimble R6 model Real Time Kinematic (RTK) GPS. Surveys were taken as one long profile along the thalweg and three fixed cross sections across the entrance channel (Figure 3). Cross sections were spaced 5 to 10 m apart from each other moving landward up the channel from the berm position (Figure 3). Survey data was post processed using Trimble Business Centre™ Version 3.8 software with each survey corrected to Australian Height Datum (AHD) through three control points referenced to at least two permanent benchmarks established by RTK GPS. For each individual opening event, the first survey was taken in the 24 hours prior to opening. Artificial opening events were focused on as this allowed monitoring to occur from the precise moment of opening. In addition, the majority of IOCE globally have entrances which are managed, meaning that human removal of the berm is a primary agent of lagoon opening. A daily record of entrance condition was obtained using multiple automated Uway VH200B Black Flash model

cameras at the Aire and Gellibrand Rivers recording an image once every two hours to support morphological observations.

Pressure sensors (Solinist Levelogger 30001) were anchored to the channel bed at four sites; (i) at the mouth, and then (ii) 200 - 300 m, (iii) 500 m, and (iv) 1.20 - 1.80 km inland of the mouth, the last within the estuarine lagoon (Figure 3). Data was logged at frequency of 0.2 Hz to allow for maximum data storage and to capture long-period wave fluctuations (e.g. tidal influence). A barometric pressure logger (Barologger 30001) was installed within a 2 km radius of all water level loggers. Mean hourly water depth (corrected to MSL) for the Gellibrand and Anglesea estuaries was supplemented from the Department of Land, Water and Planning (DELWP) Victoria's automated gauging stations (Figure 3). This data was unavailable for the Aire River. Offshore tidal data was sourced from the Bureau of Meteorology (BoM). Rainfall and upstream river discharge observations were sourced from the nearest meteorological (BoM) and flow gauging stations (DELWP), all within 7 km of the estuary mouth (Figure 2). Wave data was hindcast from National Oceanic and Atmospheric Administration's (NOAA) WAVEWATCH III model as no permanent wave buoys are present in west Victoria and no nearshore wave data was available. Grid points from WAVEWATCH III were taken at the closest possible location to the estuary entrance for each site, all being within 40 km offshore (Figure 2). Wave data was analysed using MatLab R2015 software to output the significant wave height (Hs), primary peak spectral wave period (Tp), and average direction at the peak period (Dp). From this dataset mean daily wave data was calculated and presented as a time series.

Data from the average wave conditions on the day of closure was used to estimate

the longshore drift volume delivered to the channel at the time of closure. Snell's law (Equation 1) was used to determine the nearshore wave direction (sinα):

$$\sin \alpha = \frac{C}{C_O} \sin \alpha_o \quad (1)$$

where $\sin\alpha_0$ is the angle of wave approach in deep water, C_o is deep water wave celerity (m/s), and C is nearshore wave celerity (m/s). Bathymetric contours were created from the Victorian Coastal Nearshore Bathymetry 20 m resolution DEM dataset (DELWP, 2017) on ARC GIS Version 10.3.1. Contours were traced as straight lines at the breaker position adjacent to the estuary mouth with the orientation calculated using the linear mean direction tool. A perpendicular line was cast offshore at the midpoint of the mean orientation line to represent shore normal with the azimuth measured on ARC GIS as relative to north. To account for the influence of wave breaking in the nearshore, a transformation of offshore Hs to breaking wave height (H_b) was calculated as per Holmes (2001); Masselink and Hughes (2003) (Equation 2):

$$H_b = (\frac{1}{2\pi} \frac{Co}{C})^{\frac{1}{2}} (\frac{bo}{b})^{\frac{1}{2}} H_o = K_s K_r \quad (2)$$

whereby H_o is offshore significant wave height, C_o is deep water wave celerity (m/s), C is nearshore wave celerity (m/s), b is the spacing between wave rays (determined by $b_1/b_2 = \cos \alpha_1/\cos \alpha_2$), K_s is the shoaling coefficient, and K_r is the refraction coefficient. Longshore drift was calculated using a MatLab script from Ruiz (2009) that output the immersed longshore transport rate (I_l) (in kg/s) and transformed this value to a volume transport rate (Q_l) (in m^3/day). Longshore drift was calculated using two

equations, the first being the widely used CERC formula (US Army Corp. of Engineers (USAC, 1984) (Equation 3), and the second being the Kamphuis (1991) formula (Equation 4) which includes grain size and beach slope. As the CERC equation has sometimes been known to overestimate the rate of longshore transport (Abadie et al., 2006) the results from both formulas were used for comparison. Using the CERC formula (USAC, 1984), the longshore transport rate is calculated as per Equation 3:

$$Q = \frac{k_l}{16\sqrt{\gamma}} pg_2^3 H_{sb}{}_2^5 \sin(2\theta_b) \quad (3)$$

where k = 0.39 (as recommended by USAC, 1984), y = breaker index, g = gravity (9.81), H_{sb} = Hs at breaking, p = density of water, θ_b is wave breaker angle (°).

Using the Kamphuis (1991) formula (Equation 4), the longshore transport rate is calculated as:

$$Q = 2.27(H_{sb}{}^2 T^{1.5} m^{0.75} d^{-0.25} \sin{}^{0.6}(2\theta_b) \quad (4)$$

in which H_{sb} = Hs at breaking, m = beach slope, d = sediment D_{50}, and θ_b is wave breaker angle (°). For the D_{50}, grain size samples were taken at each site and processed using a Beckman Coulter LP 13320 laser particle sizer. It is recognised that due to a lack of detailed nearshore modelling and bathymetric analysis, which was outside the scope of this study, the nearshore wave and longshore drift calculations represent approximations only due to the assumption of refraction over plane and parallel contours.

Results

Anglesea

During the period of opening at Anglesea River (14/02/2014 - 21/02/2014), deep-water waves approached from the SW (Dp offshore = 217 - 237 °N, 25 - 46 ° to the shore) with Hs ranging from 0.25 - 2.05 m and Tp 4.70 - 12.50 sec (Figure 4a-b). Wave heights peaked three days prior to closure in response to a storm 18/02 - 20/02 with an increase in Hs to >2 m (Figure 4a-b). The estuary closed on a spring tide, when the breaking wave direction was oblique to the shore (α = 25 °N), and with an estimated longshore drift rate of 322 - 374 m^3/day (Figure 4c; Table 3). No rainfall occurred throughout the opening.

Prior to opening, a berm rising to +2.37 m MSL in elevation was present at the mouth of Anglesea River (Figure 5a). On 14/02, a channel 0.32 m deep and 2.60 m wide was excavated in the center of the berm when the backing estuary water surface was at an elevation of +1.65 m MSL (Figure 4c). The excavated channel was designed to be shallow to prevent the loss of the top layer of oxygenated water and was 110 m long, with its maximum elevation occurring at +2.05 m at the position of the former berm. Throughout the first two days (14/02 - 15/02), the channel maintained a convex slope (sloping seaward at 0.42 - 0.98° from the former berm position) with minimal incision occurring (Figure 5b; Figure 6a-b). By 2 pm 15/02, the channel bed had incised to an elevation of +1.55 m MSL and the estuarine lagoon started to drain as coinciding with further widening of the channel (Figure 4c-d; Figure 5a). Throughout this time the channel maintained a rectangular cross sectional shape (Figure 5b-c; Figure 6a-c).

The channel cross section progressively incised to its lowest elevation (+0.66 m MSL) and maximum area (6.95 m^2) at the mouth on 18/02 (four days after opening) (Figure 5a). This coincided with the estuary water surface reaching a minimum elevation of +1.51 m MSL (Figure 4c). A westward lateral migration of the channel thalweg occurred from 18/02 onwards whereby a spit emerged across the mouth from the eastern side of the channel (Figure 5c-d; Figure 6c-e). At this time, water depth within the estuarine lagoon began to slowly increase (Figure 4c). The most marked change in morphology occurred between 19/02 - 21/02 when a distinct berm formed, corresponding with the period of increased deep-water Hs (Figure 4a; Figure 5a; e). The berm progressively infilled the entire channel and closed the estuary on 21/02 with its crest reaching a final elevation of +2.88 m MSL (Figure 4a; Figure 5a; Figure 6e-f). The elevation of the lagoon water surface immediately after closure was +1.54 m MSL and no tidal fluctuations were registered in the basin throughout the monitoring period (Figure 4c-d).

Gellibrand

During the period of opening at Gellibrand River (11/04/2014 - 16/12/2014), deep-water waves approached from the S - SW (Dp offshore = 182 - 245 °N, 9 - 37 ° to the shore) with Hs 0.94 - 6.00 m (Figure 7a-b). Wave heights peaked July to September in response to multiple winter storms and decreased below 2 m on average after November (Figure 7a). During June to September, the mean daily river discharge for 2014 (6.74 m^3/s) was exceeded with periods of sustained high rainfall occurring June - August (Figure 7c). Throughout this time, the estuary basin water surface fluctuated between +0.15 and +1.65 m MSL, with higher elevations occurring in association with

winter storm surges (Figure 7a-b). At the time of closure, Hs was 1.50 m with waves approaching from the SSW (Dp offshore = 211°N, α = 19°) (Figure 7a). A decrease in daily river discharge to below the mean daily flow for 2014 occurred from October - December with discharge being <1 m^3/s at the time of closure (Figure 7c). The estuary closed on a neap tidal cycle and the estimated longshore drift rate under the wave conditions on the day of closure was 959 - 975 m^3/day (Table 3).

A berm +3.79 m MSL in elevation fronted by a 5 m wide beach was present at the mouth of Gellibrand River prior to opening (Figure 8b). On 11/04, a channel 12 m wide, 48 m long and 2.65 m deep was excavated through the berm when the backing estuary water surface was +1.44 m MSL (Figure 7b; Figure 8a-b). By 9 am on 12/04, the channel bed had incised to its deepest point (-0.49 m MSL) and greatest cross sectional area (165.60 m^2) corresponding with the lagoon water surface falling to +0.20 m MSL (Figure 7b; Figure 8a-b). From 12/04 onwards, the channel thalweg shifted westward and maintained an area of deeper scour where it remained until closure (Figure 8c-g). Between 12/04 - 20/07, some infill from the eastern side of the channel occurred and the channel at the berm position accreted to +0.20 m MSL (Figure 8c-d). In response to winter high flows occurring between 20/04 - 28/10, the cross sectional area remained similar (±15 m^2) but the berm incised to -0.35 m MSL (Figure 8e-f). From 28/10 onwards, the berm steadily accreted as the daily river discharge decreased with further infill of the channel from the east (Figure 7c; Figure 8g-h). A final berm elevation of +1.33 m MSL and water depth of +0.89 m MSL was attained on 16/12 when closure occurred 249 days after opening (Figure 8g).

Aire

Monitoring of Aire River included three artificial openings and one natural opening. The first artificial opening persisted from 20/03/2014 - 11/04/2014 (21 days duration). During the monitoring period, waves approached from the SSW - SW (Dp offshore = 209 - 225º N; α = 5 - 14°), becoming more oblique on average from the 26/03 onwards. Offshore Hs was 1.80 - 5.00 m and Tp 9.50 - 15.50 sec (Figure 9a-b). The mean daily flow remained below the 2014 mean of 1.70 m^3/s aside from surpassing this by 0.20 m^3/s for two day's duration on 21/03 - 22/03 (Figure 9d). The estimated longshore drift rate under the wave conditions on the day of closure was 3,331 - 3,950 m^3/day increasing in accordance with Hs (3 m) (Table 3).

Prior to the first artificial opening, a berm +2.49 m MSL in elevation was present fronted by a 41 m wide beach (Figure 10a). On 20/03 a channel 2 m deep by 3 m wide was excavated in the center of the berm. On the 21/03, the channel reached its maximum width (182 m), cross sectional area (291 m^2), and depth at the former berm position (-0.25 m MSL) (Figure 10a-b). The basin water depth decreased steadily during in the first three days following opening before stabilizing on 24/03 (Figure 9c). Small amplitude (< 0.5 m) tidal fluctuations persisted until 08/03 (Figure 9c). While outflow dominated from 21/03 - 24/04, the excavated channel maintained a rectangular shape and a near horizontal profile (0.28 - 0.33°) infill occurring vertically and with a small amount from the east (Figure 10c). From 24/03 - 26/03, the channel thalweg diverted to the west and further infill from the east resulted in a gradual reduction in cross sectional area (Figure 10a-d). From 26/03 - 11/04, the channel bed progressively increased in elevation at a rate of +0.14 m/day (Figure 10e). The most marked change occurred between 30/03 - 03/04 during a period of increased wave height (Hs >4 m)

when a distinct berm formed to +1.32 m MSL (Figure10a). On 11/04, the channel had closed and completely infilled from the east with a final berm crest elevation of +1.55 m MSL (Figure 10a-e).

A second artificial opening was undertaken on 01/05/2014 during a storm (Hs = 4.10 - 5.10 m, Tp = 15 - 16 sec) with waves approaching form the SW - WSW (Dp offshore = 235 - 245º N; α = 1 - 3°) (Figure 9a-b). During this opening, a 5 m wide channel with a cross sectional area of 12.40 m^2 was excavated (Figure 11a-d). Within a single day the estuary had closed, and on 03/05 the resultant berm was +0.89 m higher than when the channel was cut (Figure 11e). Landward of the berm crest, the channel bed elevation also increased by +0.45 m (Figure 10e). Over the whole monitoring period, the channel infilled through vertical deposition with no migration of the thalweg or spit building evident (Figure 11a-d). The basin water depth did not decrease >0.10 m throughout the opening (Figure 9d). The estuary closed on a spring tide and the estimated longshore drift rate on the day of closure was 1,997 - 2,001 m^3/day (Table 3). Even though the Hs at closure was higher than in the first artificial opening, the calculated drift rate remained lower due to the less oblique wave direction (Table 3).

A third artificial opening was undertaken on 11/05/2014 with the estuary remaining open until 21/05/2014. During the monitoring period, Hs was 2.10 - 4.60 m (Tp = 12 - 17 sec) with waves approaching from the SSW - WSW (Dp offshore = 212 - 238º N; α = 1.50 - 13º) (Figure 9a-b). A storm with Hs >3.5 m occurred 15/05 - 18/05 (Figure 9a-b) and from 18/05 onwards, the wave direction shifted to be more oblique (α = >10°). Throughout the opening, <8 mm of rainfall occurred and the daily river discharge fluctuated within ±1 m^3/s of the 2014 mean (Figure 9d). The estuary closed on a spring

tidal cycle with an estimated longshore drift rate on the day of closure of 2,686 - 3,062 m^3/day (Figure 9c; Table 5).

Prior to the third artificial opening, the berm was +3.27 m MSL and fronted by an 18 m wide beach (Figure 12a). Within six hours of excavation, the channel reached its peak dimensions (width = 167 m, cross sectional area = 773 m^2) with a depth exceeding -2 m MSL (Figure 12a-b). The estuarine lagoon drained rapidly (0.05 m/hr) over the first 24 hours to stabilise at a minimum depth on the 13/05 (Figure 9c). While strong outflow persisted from 11/05 - 13/05, the channel maintained a rectangular shape. A decrease in channel width (91.47 m) and area (290.16 m^2) occurred by 14/05 with >2 m of accretion at the former berm position and some infill from the west (Figure 12a-c). From 14/05 - 18/05, the channel continued to increase in berm and channel bed elevation with a decrease in area (Figure 12a-d). Between 14/05 - 21/05, the channel became shallower with further lateral migration of the thalweg to the east (Figure 12d). Closure occurred on 21/05 with the berm having accreted >3.55 m since opening (Figure 9c; Figure 12a).

Three days following the last closure of Aire River, a natural opening occurred on 23/05/2014 (Figure 12a; e-g). High rainfall (40 mm between 23/05 - 25/05) increased river discharge to 2 m^3/s leading to overtopping of the berm from the catchment side (Figure 9d). Throughout the opening, Hs was between 1.80 - 4.70 m, reaching a maximum on the day of closure (Figure 9a). The estimated longshore drift rate on the day of closure was 1,905 - 2,010 m^3/day, decreasing due to a near-normal direction despite a higher Hs (Table 3). The natural opening initiated at a berm height of +1.35 m MSL when Hs was 3 m (Tp = 12.50 s) (Figure 9a; Figure 12a). Entrance breakout

commenced as a 5 mm deep flow but within two days (25/05) the channel had incised to an elevation of -0.37 m MSL at the position of the former berm (Figure 12a). The maximum channel area (291 m^2) was reached on 25/05 and the lagoon also began to decrease in water depth (Figure 9c; Figure12a). From 25/05 - 05/06 the wave height and direction fluctuated but as there was still outflow from the lagoon (>1.80 m^3/s/day), the rate of berm accretion was gradual (+0.04 m/day). By the 05/06, the channel bed at the former berm position had accreted to +0.18 m MSL with infill occurring from both sides and vertically from the channel bed (Figure 12e - f). From 05/06 onwards, Hs remained >2 m with an increase in the rate of berm deposition to +0.33m/day. The entrance closed on 11/06 (20 days after opening) at a final berm elevation of +2.16 m MSL and during a spring tidal cycle (Figure 9c; Figure12a; g).

Discussion

Controls on the rate of entrance recovery

At IOCE in Victoria, Australia, the temporal rate of berm recovery and channel infill was highly variable with entrance closures occurring between 1 and 249 days in duration as associated with event driven changes in marine and fluvial conditions rather than a long-term seasonal variability.

Waves are broadly recognised as a driver of entrance closure in IOCE through the onshore and alongshore delivery of sediment, the rate of which is known to increase in accordance with wave height (Battalio et al., 2007; Nielsen and Gordon, 2008; Wainwright et al., 2011; Rich and Keller, 2013). While storms are erosional on beaches (Lee et al., 1998; Callaghan et al., 2008), they can cause increased

sedimentation at estuary entrances as previously observed at IOCE in New South Wales, Australia (Narrabeen Lagoon: Hanslow et al., 2000; Morris and Turner, 2010), South Africa (Great Brak Estuary: Slinger, 2016), and California (Crissy Field Marsh: Hanes et al., 2011; Russian River: Behrens et al., 2013). At all IOCE in this study, wave height proved to be positively correlated to an increased rate of infill of the estuary channel (i.e. indicated by a decrease in cross sectional area) (R^2 = 0.86) and an increase in berm elevation (R^2 = 0.58) (Figure 13a-b). The breaking wave angle was negatively correlated with the rates of channel infill (R^2 = 0.83) and berm growth (R^2 = 0.60) (when assuming straight, plane nearshore bottom contours) (Figure 13c-d). In Victoria, the rapid (hourly to daily) onset of depositional processes is attributed to the year-round high energy wave conditions (Table 1). An example of this is the second artificial opening at Aire River where closure occurred within a day, when Hs was >4 m (Figure 9a; Figure 11 a-c). Wave height in western Victoria is generally >2 m year-round with net annual wave power >50 - 60 kW/m making the region one of the most high-energy coasts worldwide (Cornett, 2008; Hemer and Griffin, 2010; Hughes and Heap, 2010; Gunn and Stock-Williams, 2012). This means that provided fluvial discharge remains low-moderate relative to wave height, the extreme wave energy on the open coast is more likely to result in rapid closures of IOCE, especially at rivers that are considered small by global standards.

Higher waves did not always equate to rapid onshore sediment delivery and entrance closure. When fluvial discharge was extremely high (in the order of >four times the mean daily flow), the capacity of the ebb-tidal prism to remove sediment from the entrance exceeded the ability of waves to deliver sediment onshore. For example at the Gellibrand River, two storm surges occurred during June - August (Hs >5 m) which

temporarily increased the lagoon water depth (Figure 7a-b). Concurrently, the daily river discharge was >4 times the 2014 mean and as a result there was limited infill of the channel with the channel bed depth at the berm position remaining below MSL (Figure 7c; Figure 8e-f). This illustrates that even though wave height correlates with an increase in berm building and a decrease in channel area, it is the relative balance between wave energy and the ebb-tidal prism that determines the rate of in-channel deposition. Under lower energy wave conditions (Hs <2 m), the rates of berm and channel deposition decreased and entrance closure occurred more gradually over a weekly-monthly scale, always coinciding with periods of low river discharge (e.g. Gellibrand and Anglesea closures).

The morphodynamic observations of the study indicate that we need to revisit existing conceptual models of entrance closure processes for IOCE located on microtidal, open sandy coastlines which close several times annually. While the sites monitored in the present study can be considered representative of the majority of IOCE globally (McSweeney et al., 2017a), the study findings may not be directly applicable for seasonally open inlets. Seasonally open inlets are estuaries which close regularly once per year when seasonal variations of river flow and wave climate occur (Ranasinghe et al., 1999). IOCE in the present study closed many times throughout the year in response to individual storm events as opposed to a regular seasonal change. The entrance morphology of smaller IOCE is also known to change more rapidly over hours-days (e.g. Russian River, California: Behrens et al., 2009) compared to weeks-months at larger sites (e.g. Curdies Inlet, Australia: McSweeney et al., 2017b). This means that IOCE with larger ebb-tidal prisms than sites in the present study may show a slower ingress of marine sediment due to the relative

dominance of ebb-tidal processes. This may be a function of a higher tidal range, a larger estuary basin volume, or being located on larger catchment rivers with higher discharge under normal conditions.

Modes of closure

Analysis of the daily progression towards closure at the Anglesea, Gellibrand, and Aire River estuaries in Victoria provides evidence that two distinct modes of sedimentation exist: lateral and vertical accretion (Figure 14a-b). These two modes of entrance closure can occur in isolation or together over a single closure cycle.

Lateral accretion

Lateral accretion as a mode of entrance closure in IOCE is characterised by the growth of a spit across the entrance channel by processes of longshore drift (Figure 14a). This corresponds with descriptions of estuary entrance infill under oblique wave conditions described by Bruun and Gerritsen (1960); O'Brien and Dean (1972); Jarrett (1976); FitzGerald et al., (2000) and Ranasinghe and Pattiaratchi (2003). Lateral accretion occurred at the Gellibrand and Anglesea estuaries under lower-energy waves moving in an oblique direction (Figure 5b-e; Figure 8f-g; Table 3) and with no or very low flow in the channel. In Victoria, lateral accretion was on average a more gradual process occurring at a rate of decimeters per day and can be represented by four stages (Figure 14a). Stage 1 is entrance opening where the channel becomes connected to the ocean. Stage 2 commences when channel outflow decreases once the hydraulic head from the estuary has fallen to such a level that direct scouring of

the channel ceases. The formation of a spit in the lower channel initiates as longshore drift begins to dominate. For example, at Anglesea, spit building initiated four days following opening and only when outflow energy decreased as the basin water depth had drained to a minimum (Figure 5c; Figure 6c-d). During Stage 3, the spit continues to grow and diverts the thalweg to the far bank of the channel. Provided fluvial discharge does not increase, sediment will further infill the channel, deflect it to be shore-parallel and re-establish the berm. Stage 4 is full entrance closure. If river flow increases during Stages 2 or 3, sediment may be re eroded from the entrance which can temporarily reset the channel morphology back to Stage 1 or 2. This cycle of flood driven resetting was observed at the Gellibrand River where during the first 100 days following opening, berm accretion was evident while river discharge remained low (Figure 7c, Figure 8d). When discharge increased above the mean daily value (June to September) the berm again incised to below MSL (Figure 7c Figure 8f). The duration of the flood reset cycle is dependent on the magnitude and duration of the flood. Similar entrance closure by emergence of a spit in the direction of longshore drift have been described at seasonally open estuaries in Vietnam (Tund et al., 2006) and Western Australia (Wilson Inlet: Ranasinghe and Pattiaratchi, 2003) specifically in conjunction with the onset of seasonal low river flows. Longshore drift is known to be most efficient at delivering sediment to beaches when the angle of approach relative to the shoreline is between 32 - 45° (Siegle and Asp, 2007). In Victoria, spit building resulting in closure occurred when the nearshore wave direction (α) was 19 - 45° (Anglesea and Gellibrand closures) and only when river discharge was below the mean daily flow.

Vertical accretion

Vertical accretion as a mechanism of closure is characterised by rapid berm and channel bed accretion under higher swells (Hs >2 m) from a more shore-normal direction (Figure 14b). In this instance, sediment infills the entrance channel vertically from the channel bed without any lateral migration of the thalweg occurring. Rapid berm growth on beaches and estuary entrances during high-energy wave conditions can occur by increased deposition through swash uprush and overtopping at the position of the existing berm crest (Baldock et al., 2005; Weir et al., 2006; Matias et al., 2010). During vertical accretion, wave uprush with swash overtopping at the landward extent of the berm is the primary mode of deposition. This is evident by the increase in channel elevation landward of the berm crest (Figure 11e). The more rapid rate of deposition is likely due to: (1) an increased rate of entrainment and onshore sediment delivery from high energy swell waves, (2) a further landward deposition limit with increased wave height, and (3) a more shore normal wave direction providing a more direct transfer of energy into the channel (Weir et al., 2006; Morris and Turner, 2007; Baldock et al., 2008). Aire River following the second artificial opening provides an example of vertical accretion with the channel bed showing no lateral migration. Throughout the opening, Hs was >4 m and the wave direction remained within 3º of shore normal (Figure 11a-e; Table 3). Additionally, this closure was coupled with a spring tide which likely increased the landward extent of deposition beyond the berm crest due to a higher nearshore water level (Figure 9c). A similar example is the East Kleinemonde estuary, South Africa, which closes within a few tidal cycles during near shore-normal, high-energy wave conditions adjacent to the mouth (Whitfield et al., 2008) and Crissy Marsh, California, which also tends to close under successively increasing high tides (Hanes et al., 2011). Cross-shore transport is recognised as a

mechanism of closure at IOCE on embayed beaches during long period, near-normal swell incidence (Cooper, 1994; Ranasinghe and Pattarachi, 2003; Tund et al., 2006) however closure always corresponded with seasonal decreases in streamflow. In these instances, sediment is sourced from an offshore bar consisting of sand eroded during entrance opening (Ranasinghe et al., 1999; Ranasinghe and Pattiaratchi, 2003). Closure by vertical accretion at Aire River occurred under winter streamflow and wave conditions which suggests that it may also be a function of individual high-energy wave events as opposed to a gradual, seasonal process. Vertical accretion was limited as a mode of closure to Aire River, a headland bound estuary with a short beach (1 km) and with a small tidal prism (4.6×10^6 m^3). Similarly, cross-shore processes have previously been described as most influential at IOCE on embayed beaches (Ranasinghe et al., 1999; Harley et al., 2011).

Lateral and vertical accretion do not necessarily occur in isolation. Field observations at IOCE in Victoria show that these processes can combine to infill the entrance channel over a single closure cycle. The switch between these modes of deposition is related to event driven variations in the wave climate and fluvial discharge. For example, at Aire River following the first artificial opening, the morphological change in the channel and wave conditions transitioned between those characteristic of both lateral and rapid vertical accretion (Figure 9; Figure 10). In the first week following opening, the wave direction was more normal to the shore (α = <6°) with rapid channel bed accretion (Figure 10b-c) but during 26/03/2014 - 11/04/2014, the wave direction shifted to be more oblique (α = >10°) with channel infill becoming dominated by lateral accretion and eastward channel migration (Figure 10d-e).

Entrance opening duration

The duration of entrance opening was not a function of the basin water depth at the time of opening or the maximum channel dimensions, but the relative balance of ebb-tidal to wave energy once the lagoon had ceased draining (i.e. removal of hydraulic head). This was evident following the third artificial opening at Aire River, where the estuary only remained open for 11 days despite having the largest channel dimensions attained following opening (cross sectional area = 773 m^2 and depth = > -2 m MSL) (Figure 12a). This was due to sustained high waves (Hs >3 m) with limited fluvial discharge throughout the opening period (Figure 9a-d). In contrast, the Gellibrand River remained open for 249 days despite multiple winter storms that may otherwise close the entrance as the mean daily flow was exceeded for several months (Figure 7c). A similar observation is described for Wilson Inlet (Western Australia) where streamflow, if sufficiently strong, can overcome the depositional effects of storms (Ranasinghe and Pattaratchi, 2003). This highlights the importance of event driven change in fluvial conditions and the ebb-tidal prism as a control on the entrance opening duration.

While wave height and the ebb-tidal flow are the main factors controlling the morphological evolution of IOCE, the tidal water level may also play a role in the timing of entrance closure. The tidal cycle is not often considered in terms of its direct impact on closure processes, but mainly as a mechanism of improving water circulation within the lagoon (Gale et al., 2006). No consistent correlation has been shown between tidal elevation and the timing of entrance closures in existing literature (Whitfield et al., 2008; Hanes et al., 2011; Behrens et al., 2013). In the present study, two thirds of

closures coincided with a spring tidal cycle (Gellibrand and the first Aire artificial opening occurred on neaps) (Figure 4e; Figure 7b; Figure 9c). While a detailed analysis of tidal processes was not a main focus of this study, there is potential that spring tides may provide an additional forcing factor for entrance closures during low flows and following the initial onset of berm building. A higher nearshore water level is known to increase the wave runup limit and cross shore deposition further landward, particularly at embayed beaches (Weir et al., 2006; Salmon et al., 2007; Phillips et al., 2017). Spring tidal pumping is often described during entrance opening whereby the larger tidal forcing of the spring tide increases lagoon water levels (Hinwood et al., 2005; McLean and Hinwood, 2011). In the present study, lagoonal tidal fluctuations did not occur at Anglesea which indicates that a long, shallow channel can provide sufficient resistance to inhibit tidal propagation into the basin, even during spring tides (Figure 4c-d; Figure 6a-f). The lack of tidal exchange means that the opening may have a limited impact in improving water quality and exchange.

Conclusions

Daily scale monitoring following entrance openings at IOCE on an open microtidal, sandy coast shows two distinct modes of entrance closure: (a) lateral accretion, whereby the estuary closes by longshore drift-driven spit growth under low river flows, and (b) vertical accretion, where the channel aggrades under high (>2 m), near-normal waves (i.e. cross-shore transport). Although the interaction of cross-shore and longshore drift processes with ebb-tidal currents has been previously described as closure mechanisms in seasonally open estuaries (e.g. Wilson Inlet, Western Australia: Ranasinghe and Pattiaratchi, 2003), both processes were observed to close

IOCE over a more rapid temporal scale (daily-weekly) in Victoria, Australia. A key distinction is that in Victoria, entrance closures occurred all year-round and independent of sustained seasonal variations in river discharge and wave height. This is attributed to the wave climate being one of the highest energy regions globally where wave-driven deposition may overcome even moderate river flows, especially at IOCE with small tidal prisms. Lateral and vertical accretion were also observed to operate concurrently in association with changing fluvial and marine conditions during an individual closure cycle. Although wave height showed a strong positive correlation with the rate of channel infill and berm building, when fluvial discharge and wave height simultaneously increase, as is typical during winter storms, high swells will not always close the mouth due to the increased ebb-tidal prism. As estuaries in the present study are representative of the majority of IOCE globally (McSweeney et al., 2017a), the models of closure processes are therefore applicable worldwide. Incorporating a detailed nearshore analysis of wave conditions would be valuable to refine these models in the future to examine processes such as wave refraction more comprehensively (Hanes and Erikson, 2013).

This present study provides coastal managers with a better understanding of the conditions that promote rapid entrance closure in IOCE. This can save considerable time and money in deciding when to implement artificial openings. Although there is substantial pressure to artificially open IOCE to alleviate flooding and poor water quality, this study highlights the importance of forecasting fluvial and marine conditions in the days-weeks following an opening. To avoid rapid reclosure, artificial openings should not be implemented during large swells regardless of how high basin water levels are and particularly in the absence of forecast sustained high river discharge.

Ideal conditions for a sustained opening (at least weeks in duration) would include during low waves (H_s <2 m) and immediately preceding high rainfall and river discharge. The basin water level is often used as an indicator of when to artificially open an estuary entrance. While a higher water level may be related to larger channel dimensions, and is important for short-term flood alleviation, the marine and fluvial conditions after the estuary has drained to a minimum depth are most critical in determining the opening duration. The forecast geomorphic conditions should therefore be considered in existing decision support tools for artificial entrance openings.

Acknowledgements

The Victorian Department of Environment, Land, Water and Planning (DELWP) is thanked for providing financial support for this project. The lead author was supported by an Australian Postgraduate Award from The University of Melbourne and a Science Postgraduate Writing up Award. Estuary Watch Victoria is also thanked for entrance condition records for the Gellibrand and Anglesea Rivers and Neville Rosengren is thanked for images of the study sites. We thank the reviewers for their helpful comments which have improved the quality of the manuscript.

References

Abadie S, Bute, R., Mauriet S, Morichon D, Dupuis H. 2006. Wave climate and longshore drift on the South Aquitaine coast. Continental Shelf Research, 26(16), 1924-1939.

Aleman N, Robin N, Certain R, Anthony EJ, Barusseau, JP. 2015. Longshore variability of beach states and bar types in a microtidal, storm-influenced, low-energy environment. Geomorphology 241: 175-191

Aubrey D, Gaines AG. 1982. Rapid formation and degradation of barrier spits in areas with low rates of littoral drift. Marine Geology 49: 257-277

Baldock T, Hughes MG, Day K, Louys J. 2005. Swash overtopping and sediment overwash on a truncated beach. Coastal Engineering 52: 633-645

Baldock T, Weir F, Hughes MG. 2008. Morphodynamic evolution of a coastal lagoon entrance during swash overwash. Geomorphology 95: 398-411

Barton J, Sherwood JE. 2004. Estuary opening management in Western Victoria: An information analysis. Parks Victoria Melbourne: Victoria.

Battalio B, Danmeier D, Williams P. 2007. Predicting closure and breaching frequencies of small tidal inlets - a quantified conceptual model. In Coastal Engineering 2006: (In 5 Volumes). World Scientific; 3937-3949.

Behrens DK, Bombardelli FA, Largier JL, Twohy E. 2009. Characterization of time and spatial scales of a migrating rivermouth. Geophysical Research Letters, 36(9).

Behrens D, Bombardelli FA, Largier JL, Twohy E. 2013. Episodic closure of the tidal inlet at the mouth of the Russian River - A small bar-built estuary in California. Geomorphology 189: 66-80

Bruun P, Gerritsen F. 1960. Stability of coastal inlets. Coastal Engineering Proceedings 1: 23

Callaghan D, Nielsen P, Short A, Ranasinghe R. 2008. Statistical simulation of wave climate and extreme beach erosion. Coastal Engineering 55: 375-390

Cooper J. 1994. Sedimentary processes in the river-dominated Mvoti estuary, South Africa. Geomorphology 9: 271-300

Cooper J. 2001. Geomorphological variability among microtidal estuaries from the wave-dominated South African coast. Geomorphology 40: 99-122

Cornett AM. 2008. A global wave energy resource assessment. In The Eighteenth International Offshore and Polar Engineering Conference. International Society of Offshore and Polar Engineers.

Davis Jr RA. 1989. Texture, composition and provenance of beach sands, Victoria, Australia. Journal of coastal research, 37-47.

Dept. of Land, Water and Environmental Planning (DELWP). 2017. Victorian Coastal Nearshore Bathymetry 20 m resolution DEM. Retrieved 20/03/2017 from: http://services.land.vic.gov.au/catalogue/metadata?anzlicId=ANZVI0803004748&publicId=guest&extractionProviderId=1

Estuary Watch Victoria. 2017. Database of estuary entrance observations. Data retrieved 25/01/2016 from: www.estuarywatch.org.au.

FitzGerald D. 1988. Shoreline erosional-depositional processes associated with tidal inlets. In Hydrodynamics and sediment dynamics of tidal inlets. Springer; 186-225.

FitzGerald D, Kraus NC, Hands EB. 2000. Natural mechanisms of sediment bypassing at tidal inlets. DTIC Document: Vicksburg MS Coastal and Hydraulics Lab.

Fortunato A, Nahon A, Dodet G, Pires AR, Freitas MC, Bruneau N, Azevedo A, Bertin X, Benevides P, Andrade C. 2014. Morphological evolution of an ephemeral tidal inlet from opening to closure: the Albufeira inlet, Portugal. Continental Shelf Research 73: 49-63

Gale E, Pattiaratchi C, Ranasinghe R. 2006. Vertical mixing processes in intermittently closed and open lakes and lagoons, and the dissolved oxygen response. Estuarine, Coastal and Shelf Science 69: 205-216

Gao S, Collins M. 1994. Tidal inlet equilibrium, in relation to cross-sectional area and sediment transport patterns. Estuarine, Coastal and Shelf Science 38: 157-172

Garside C, Glasby TM, Coleman MA, Kelaher BP, Bishop MJ. 2014. The frequency of connection of coastal water bodies to the ocean predicts Carcinus maenas invasion. Limnology and Oceanography 59: 1288-1296

Gunn K, Stock-Williams C. 2012. Quantifying the global wave power resource. Renewable Energy 44: 296-304

Hanes D, Ward K, Erikson LH. 2011. Waves and tides responsible for the intermittent closure of the entrance of a small, sheltered tidal wetland at San Francisco, CA. Continental Shelf Research 31: 1682-1687

Hanes DM, Erikson LH. 2013. The significance of ultra-refracted surface gravity waves on sheltered coasts, with application to San Francisco Bay. Estuarine, Coastal and Shelf Science, 133, 129-136.

Hanslow D, Davis GA, You BZ, Zastawny J. 2000. Berm height at coastal lagoon entrances in NSW. In Proc. 10th Annual. NSW Coastal Conference, Yamba.

Harley M, Turner IL, Short AD, Ranasinghe R. 2011. Assessment and integration of conventional, RTK-GPS and image-derived beach survey methods for daily to decadal coastal monitoring. Coastal Engineering 58: 194-205

Harris PT, Heap AD, Bryce SM, Porter-Smith R, Ryan DA, Heggie DT. 2002. Classification of Australian clastic coastal depositional environments based upon a quantitative analysis of wave, tidal, and river power. Journal of Sedimentary Research, 72(6), 858-870.

Hemer M, Griffin DA. 2010. The wave energy resource along Australia's southern margin. Journal of Renewable and Sustainable Energy 2: 043108

Hinwood J, McLean E, Trevethan M. 2005. Spring tidal pumping. In Coasts and Ports 2005: Coastal Living-Living Coast; Australasian Conference; Proceedings (p. 601). Institution of Engineers, Australia.

Hinwood J, McLean EJ. 2015. Predicting the dynamics of intermittently closed/open estuaries using attractors. Coastal Engineering 99: 64-72

Hodgkin EP, Hesp P. 1998. Estuaries to salt lakes: Holocene transformation of the estuarine ecosystems of south-western Australia. Marine and Freshwater Research, 49(3), 183-201.

Holmes P. 2001. Coastal Infrastructure Design, Construction and Maintenance. Department of Civil and Environment Engineering, Imperial College, England.

Hughes M, Heap AD. 2010. National-scale wave energy resource assessment for Australia. Renewable Energy 35: 1783-1791

Jarrett J. 1976. Tidal prism-inlet area relationships. DTIC Document.

Jones M, West RJ. 2005. Spatial and temporal variability of seagrass fishes in intermittently closed and open coastal lakes in southeastern Australia. Estuarine, Coastal and Shelf Science 64: 277-288

Kamphuis J. 1991. Alongshore sediment transport rate. Journal of waterway, port, coastal, and ocean engineering 117: 624-640

Kench PS. 1999. Geomorphology of Australian estuaries: review and prospect. Austral Ecology, 24(4), 367-380.

Kennard M, Pusey BJ, Olden JD, MacKay SJ, Stein JL, Marsh N. 2010. Classification of natural flow regimes in Australia to support environmental flow management. Freshwater biology 55: 171-193

Largier J, Taljaard S. 1991. The dynamics of tidal intrusion, retention, and removal of seawater in a bar-built estuary. Estuarine, Coastal and Shelf Science 33: 325-338

Leatherman S. 1979. Beach and dune interactions during storm conditions. Quarterly Journal of Engineering Geology and Hydrogeology 12: 281-290

Lee G, Nicholls RJ, Birkemeier WA. 1998. Storm-driven variability of the beach-nearshore profile at Duck, North Carolina, USA, 1981–1991. Marine Geology 148: 163-177

McKenzie J, Quinn GP, Matthews TG, Barton J, Bellgrove A. 2011. Influence of intermittent estuary outflow on coastal sediments of adjacent sandy beaches. Estuarine, Coastal and Shelf Science 92: 59-69

McLean EJ, Hinwood JB. 2011. Spring tidal pumping. In Proceedings of the 34th World Congress of the International Association for Hydro-Environment Research and Engineering: 33rd Hydrology and Water Resources Symposium and 10th Conference on Hydraulics in Water Engineering (p. 1109). Engineers Australia.

McSweeney SL, Kennedy DM, Rutherfurd ID, Stout JC. 2017a. Intermittently Closed/Open Lakes and Lagoons: Their global distribution and boundary conditions. Geomorphology, 292, 142-152.

McSweeney SL, Kennedy DM, Rutherfurd ID. 2017b. A geomorphic classification of intermittently open/closed estuaries (IOCE) derived from estuaries in Victoria, Australia. Progress in Physical Geography, DOI: 0309133317709745.

Matias A, Ferreira Ó, Vila-Concejo A, Morris B, Dias JA. 2010. Short-term morphodynamics of non-storm overwash. Marine Geology 274: 69-84

Milliman JD, Syvitski JP. 1992. Geomorphic/tectonic control of sediment discharge to the ocean: the importance of small mountainous rivers. The Journal of Geology, 100(5), 525-544.

Mondon J, Sherwood J, Chandler F. 2003. Western Victorian estuaries classification project. In Report to the Western Coastal Board pp136.

Monge-Ganuzas M, Evans G, Cearreta A. 2015. Sand-spit accumulations at the mouths of the eastern Cantabrian estuaries: The example of the Oka estuary (Urdaibai Biosphere Reserve). Quaternary International 364: 206-216

Morris B, Turner IL. 2010. Morphodynamics of intermittently open–closed coastal lagoon entrances: new insights and a conceptual model. Marine Geology 271: 55-66

Neira J, Potter IC. 1992. Movement of larval fishes through the entrance channel of a seasonally open estuary in Western Australia. Estuarine, Coastal and Shelf Science 35: 213-224

Nichol SL, Boyd R, Penland S. 1994., Stratigraphic response of wave-dominated estuaries to different relative sea-level and sediment supply histories: Quaternary case studies from Nova Scotia, Louisiana and Eastern Australia, in Dalrymple, R.W., Boyd, R., Zaitlin, B.A., eds. Incised-Valley Systems: Origin and Sedimentary Sequences: SEPM, Special Publication 51, p. 265–283.

Nielsen A, Gordon AD. 2008. The hydraulic stability of some large NSW estuaries. Australian Journal of Civil Engineering 5: 49-60

Nordstrom K, Jackson NL, Allen JR, Sherman DJ. 2003. Longshore sediment transport rates on a microtidal estuarine beach. Journal of waterway, port, coastal, and ocean engineering 129: 1-4

O'Brien M, Dean RG. 1972. Hydraulics and sedimentary stability of coastal inlets. In Coastal Engineering; 761-780.

O'Neill K, Schreider M, McArthur L, Schreider S. 2015. Changes in the water quality characteristics during a macroalgal bloom in a coastal lagoon. Ocean & Coastal Management 118: 32-36

Perissinotto R, Stretch DD, Whitfield AK, Adams JB, Forbes AT, Demetriades NT. 2010. Temporarily open/closed estuaries in South Africa. Nova Science Publishers, New York.

Phillips MS, Blenkinsopp CE, Splinter KD, Harley MD, Turner IL, Cox RJ. 2017. High-frequency observations of berm recovery using a continuous scanning Lidar. Australasian Coasts & Ports 2017: Working with Nature, 872.

Pope A. 2011. Investigation of Anglesea River estuary mouth dynamics: Review and recommendations for estuary management. School of Life and Environmental Sciences, Deakin University, Warrnambool, Vic.

Puckridge J, Sheldon F, Walker KF, Boulton AJ. 1998. Flow variability and the ecology of large rivers. Marine and freshwater research 49: 55-72

Ranasinghe R, Pattiaratchi C, Masselink G. 1999. A morphodynamic model to simulate the seasonal closure of tidal inlets. Coastal Engineering 37: 1-36

Ranasinghe R, Pattiaratchi C. 1999. The seasonal closure of tidal inlets: Wilson Inlet - a case study. Coastal Engineering 37: 37-56

Ranasinghe R, Pattiaratchi C. 2003. The seasonal closure of tidal inlets: causes and effects. Coastal Engineering Journal 45: 601-627

Ranasinghe R, Duong TM, Uhlenbrook S, Roelvink D, Stive M. 2013. Climate-change impact assessment for inlet-interrupted coastlines. Nature Climate Change 3: 83-87

Rich A, Keller EA. 2013. A hydrologic and geomorphic model of estuary breaching and closure. Geomorphology 191: 64-74

Risbey J, Pook MJ, McIntosh PC, Wheeler MC, Hendon HH. 2009. On the remote drivers of rainfall variability in Australia. Monthly Weather Review 137: 3233-3253

Roy P, Williams RJ, Jones AR, Yassini I, Gibbs PJ, Coates B, West RJ, Scanes, PR, Hudson, JP, Nichol, S. 2001. Structure and function of south-east Australian estuaries. Estuarine, Coastal and Shelf Science 53: 351-384

Ruiz G. 2009. Longshore Sand Transport (LST) Version 1.1. Code for MatLab R2015b. Retrieved 20/01/2017 from: https://au.mathworks.com/matlabcentral/fileexchange/24896-longshore-sand-transport--lst-?s_tid=srchtitle (MATLAB Central File Exchange)

Salmon SA, Bryan KR, Coco G. 2007. The use of video systems to measure run-up on beaches. Journal of Coastal Research, 50, 211-215.

Sharley D, Amos C, Pettigrove V. 2012. Factors Affecting the Ecology of the Anglesea River. Final Report for the Corangamite Catchment Management Authority: Victoria, Australia.

Siegle E, Asp NE. 2007. Wave refraction and longshore transport patterns along the southern Santa Catarina coast. Brazilian Journal of Oceanography 55: 109-120

Slinger J. 2016. Hydro-morphological modelling of small, wave-dominated estuaries. Estuarine, Coastal and Shelf Science:

Snow G, Taljaard, S. 2007. Water quality in South African temporarily open/closed estuaries: a conceptual model. African Journal of Aquatic Science 32: 99-111

Treloar P, Roper AM, Smith GP. 1993. Lake Illawarra-Numerical Modelling of Entrance Processes. In 11th Australasian Conference on Coastal and Ocean Engineering: Coastal Engineering a Partnership with Nature; Preprints of Papers. Institution of Engineers, Australia; 617.

Tunbridge B, Glenane TJ. 1988. A study of environmental flows necessary to maintain fish populations in the Gellibrand River and estuary [Victoria]. In Technical Report Series - Arthur Rylah Institute for Environmental Research (Australia).

Tund T, Cat VM, Thanh LD. 2006. Conceptual model of seasonal opening/closure of tidal inlets and estuaries at the central coast of Vietnam. In Vietnam–Japan Estuary Workshop; 157-162.

US Army Corp. Of Engineers. (USACE). 1984. Shore Protection Manual 4th edition. Department of the Army Waterways Experiment Station. US Government Printing Office, Washington, DC.

Vu T, Nielsen P, Callaghan DP. 2014. Morphology of coastal lagoon entrances: waves versus tides. Coastal Engineering Proceedings 1: 89

Wainwright D, Kidd LJ, Guard PA, Baldock TE. 2011. Morphodynamic modelling of entrance breakout for a coastal lake. In Coasts and Ports 2011: Diverse and Developing: Proceedings of the 20th Australasian Coastal and Ocean Engineering Conference and the 13th Australasian Port and Harbour Conference. Engineers Australia; 756.

Walton T, Dean RG. 2010. Longshore sediment transport via littoral drift rose. Ocean Engineering 37(2): 228-235

Weir F, Hughes MG, Baldock TE. 2006. Beach face and berm morphodynamics fronting a coastal lagoon. Geomorphology 82: 331-346

Whitfield A, Adams JB, Bate GC, Bezuidenhout K, Bornman TG, Cowley PD, Froneman PW, Gama PT, James NC, Mackenzie B. 2008. A multidisciplinary study of a small, temporarily open/closed South African estuary, with particular emphasis on the influence of mouth state on the ecology of the system. African Journal of Marine Science 30: 453-473

Whitfield A, Bate GC, Adams JB, Cowley PD, Froneman PW, Gama PT, Strydom NA, Taljaard, S, Theron AK, Turpie JK. 2012. A review of the ecology and management of temporarily open/closed estuaries in South Africa, with particular emphasis on river flow and mouth state as primary drivers of these systems. African Journal of Marine Science 34: 163-180

Table 1: Wave statistics for the west Victorian coast. Data is taken from the Port Campbell wave buoy deployed 2011 - 2013 at 38.43°S, 142.47°E in 60 m depth (Sustainability Victoria, 2013). The buoy is within a 60 km radius of all sites. Hmax = maximum wave height; Hs = significant wave height; Tz = zero crossing period; Tp = primary peak spectral wave period; Dp. = average direction at the peak period.

Month	Hmax (m)	Hs (m)	Tz (secs)	Tp (secs)	Dp (° from N)
Jan	3.69	2.22	7.29	11.79	211.51
Feb	3.65	2.20	7.47	11.67	203.48
Mar	3.95	2.37	7.51	12.34	209.67
Apr	4.20	2.55	8.21	13.09	210.08
May	4.46	2.71	7.94	12.96	211.92
Jun	4.59	2.77	7.54	12.67	214.46
July	4.45	2.70	7.58	12.92	214.48
Aug	4.46	2.70	7.74	13.18	221.46
Sep	4.84	2.94	8.10	13.26	217.85
Oct	4.19	2.54	8.04	12.71	213.42
Nov	3.41	1.97	7.23	11.89	216.53
Dec	3.69	2.23	7.14	11.64	208.61
Mean Annual	4.13	2.49	7.65	12.51	212.79

Table 2: Summary of entrance opening events and number of surveys at the study sites. T_o is time of opening and T_{CL} is time of closure.

Site and opening event	T_O (date)	T_{CL} (date)	Opening duration	Number of surveys
Anglesea	14/02/14	21/02/14	8 days	16
Gellibrand	11/04/14	16/12/14	249 days	18
Aire (artificial opening 1)	20/03/14	11/04/14	21 days	10
Aire (artificial opening 2)	01/05/14	02/05/14	1 day	6
Aire (artificial opening 3)	11/05/14	21/05/14	11 days	8
Aire (natural opening)	23/05/14	10/06/14	20 days	4

Table 3: Hs, Tp, Dp, α_0 (offshore wave angle relative to contours), α (breaking wave angle), and estimated daily total longshore drift rate (Q) at all study sites under the wave conditions on the time of closure. Drift rate is approximate only and is calculated using equations by USACE (1984) (CERC equation) and Kamphuis (1991). Wave data hindcast from NOAA Wave Watch III model.

Site	Anglesea	Gellibrand	Aire (AO1)	Aire 2 (AO2)	Aire 3 (AO3)	Aire (NO)
Closure date	21/02/14	16/12/14	11/04/14	02/05/14	21/05/14	10/06/14
Hs (m)	0.80	1.50	3	4.10	3.20	4.70
Tp (sec)	11.50	10.50	12	16	12.41	14
Dp (°N)	218	211	209	245	222	230
α_0 (°)	66	30	29	7	25	6
α (°)	25	19	14	3	11	2.20
Q (m^3/day) (CERC)	374	975	3950	1997	3062	1905
Q (m^3/day) (Kamphuis)	322	959	3331	2001	2686	2010

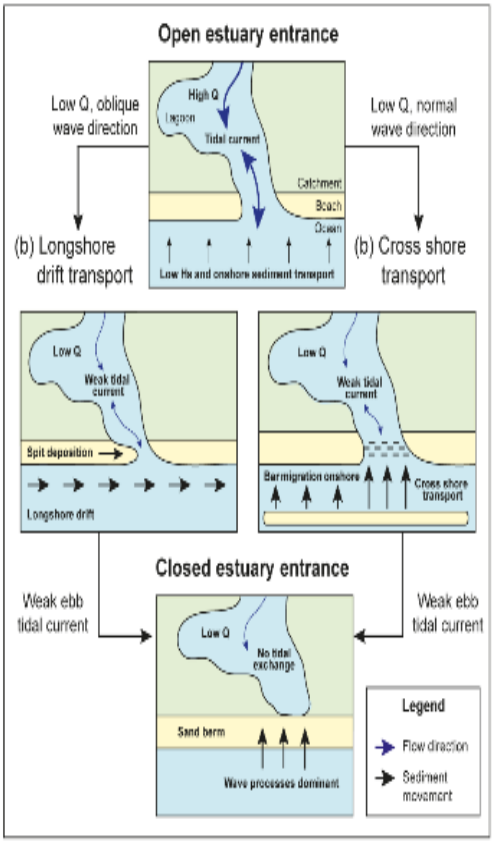

Figure 1. Conceptual model of entrance closure processes in IOCE. After known mechanisms of closure in seasonally open inlets from Ranasinghe and Pattiaratchi, 1999a; 2003. Q refers to fluvial discharge.

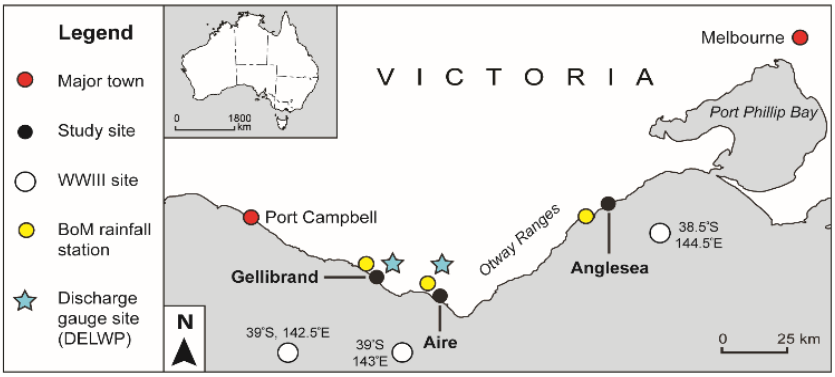

Figure 2. Location of study sites (Gellibrand, Aire and Anglesea estuaries) in Victoria, Australia. Grid points from wave data hindcasting are shown, as well as rainfall and fluvial discharge monitoring sites (from the Department of Land, Water and Environmental Planning (DELWP), Victoria).

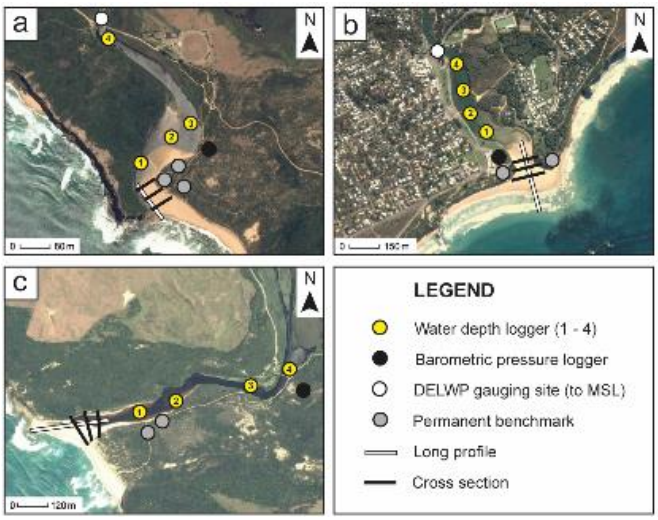

Figure 3. Study site instrumentation showing the placement of water depth and barometric pressure loggers, survey and permanent benchmark locations, and automated estuary basin water level gauging sites (from DELWP). (a) Gellibrand River; (b) Anglesea River; and (c) Aire River.

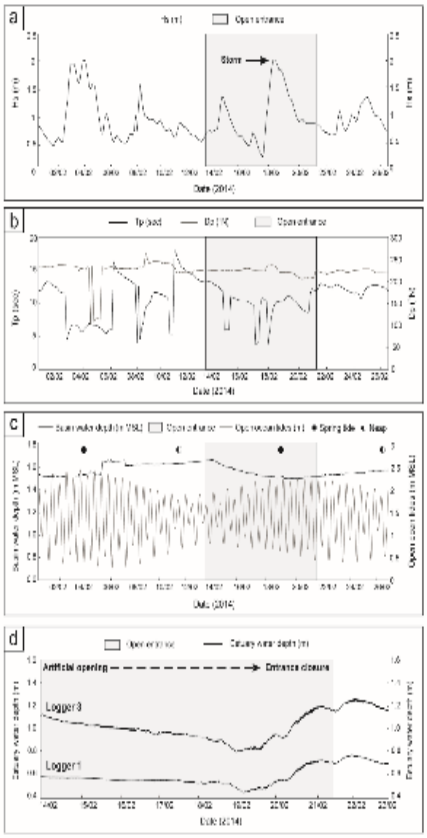

Figure 4. Marine and fluvial conditions at Anglesea River prior to and throughout artificial entrance opening. Open entrance condition is shown by grey boxes. (a) Significant wave height (Hs); (b) wave period (Dp) and direction (Dp); (c) basin water depth from DELWP automated water level gauging site (site ID: 235278) (corrected to MSL) (datum: AHD, 800 m from mouth); (d) basin water depth with respect to channel bed (from depth loggers 1: mouth and 3: 500 m upstream) with no tidal fluctuations in water level observed throughout the opening period. No rainfall occurred during the study period (BoM site ID: 090180).

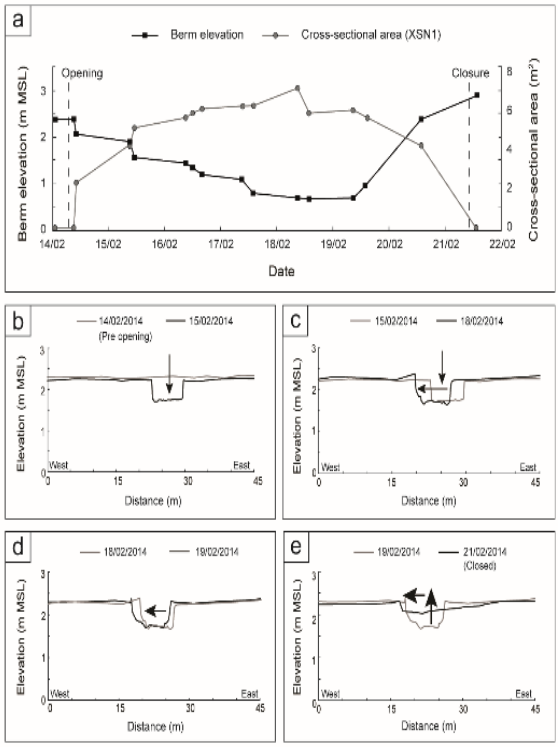

Figure 5. Change in entrance morphology at Anglesea River. (a) Change in berm elevation and cross sectional area from opening through to closure. There is a higher rate of incision at the lower cross section (XSN 1) so this was used to present cross sectional data. (b) 14/02/2014 - 15/02/2014 (pre and post entrance opening) - opening undertaken 9 am 14/02/2014). Incision is dominant. Arrow represents the direction of sediment movement and arrow size represents the magnitude of sediment movement. (c) 15/02/2014 - 18/02/2014. Initiation of spit building; (d) 18/02/2014 - 19/02/2014. Further spit building and thalweg migration. (e) 19/02/2014 - 21/02/2014. Entrance closed on 21/02/2014.

Figure 6. Photos of Anglesea artificial opening. (a) Closed estuary immediately prior to entrance opening 14/02/2014; (b) Channel excavation 10 am 14/02/2014; (c) Initial growth of lower entrance channel spit 16/02/2014; (d) Further spit development 17/02/2014; (e) Spit growth and a reduction on outflow depth 18/02/2014; (f) Further bar elongation and berm accretion 19/02/2014 prior to full entrance closure. All images taken at low tide.

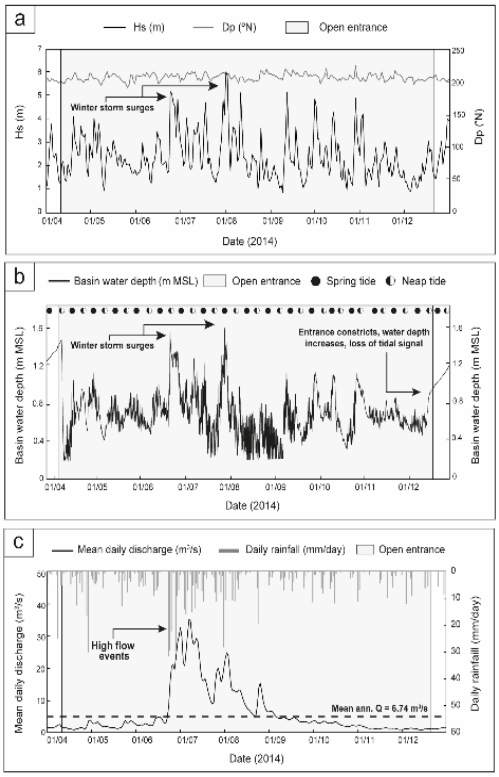

Figure 7. Marine and fluvial conditions at Gellibrand River following artificial opening. Open entrance condition is shown by grey boxes. (a) Significant wave height (Hs) and direction (Dp); (b) basin water depth from DELWP automated water level recorder (site ID: 235269) (m above MSL) (datum: AHD, 1.20 km from mouth); (c) daily rainfall (BoM site ID: 090071) and river discharge (DELWP) (site ID: 235224) with mean annual flow shown as dashed line.

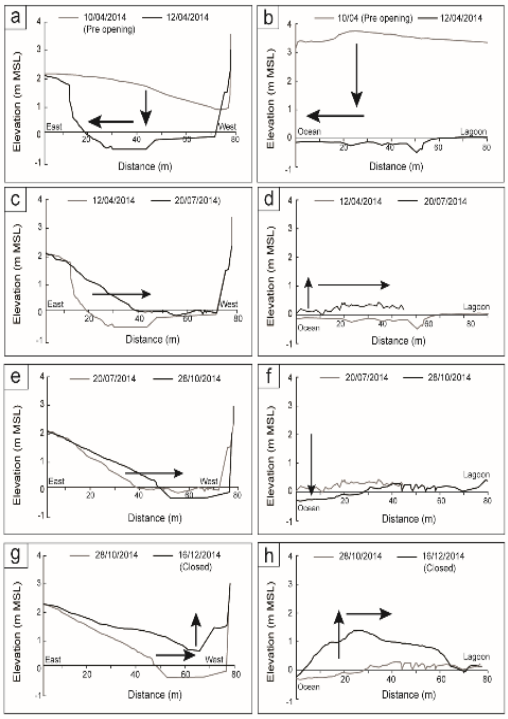

Figure 8. Change in entrance morphology at Gellibrand River following artificial opening with cross section 1 (XSN1) showing trend of morphological change. Arrows represent the direction of sediment movement with the size representing the magnitude of sediment movement. (a) Cross section. 10/04/2014 - 12/04/2014 (pre-opening - post-opening); (b) long profile 10/04/2014 - 12/04/2014; (c) 12/04/2014 - 20/07/2014 (small amount of lateral infill from east); (d) long profile 12/04/2014 - 20/07/2014; (e) cross section 20/07/2014 - 28/20/2014 (some infill from east); (f) long profile 20/07/2014 - 28/10/2014 (incision at berm position following winter high river flow); (g) cross section 28/10/2014 - 16/12/2014 (further lateral infill until closure); (h) long profile 28/20/2014 - 16/12/2014 (berm accretion).

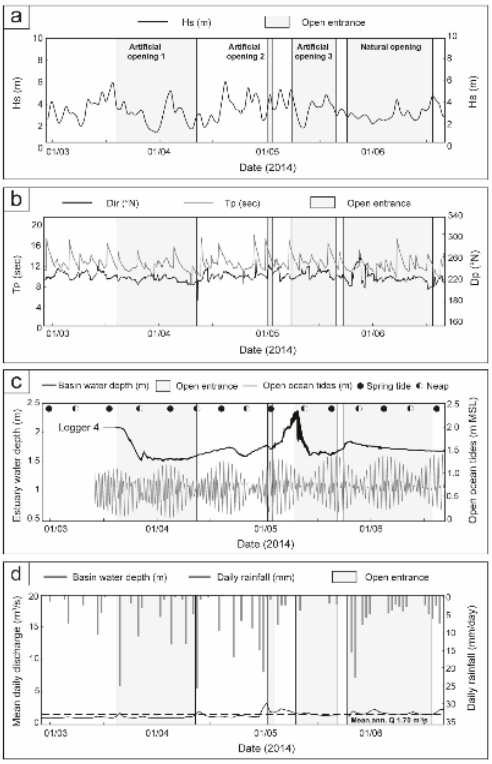

Figure 9. Marine and fluvial conditions at Aire River prior to and throughout artificial entrance opening. Open entrance condition is shown by grey boxes. (a) Significant wave height (Hs); (b) wave period (Tp) and direction (Dp); (c) basin water depth with respect to channel bed (from depth logger 4, 1.8 km upstream of mouth and open ocean tidal range; (d) daily rainfall (BoM site ID: 090093) and river discharge (DELWP) (site ID: 235219) with mean annual flow shown as dashed line.

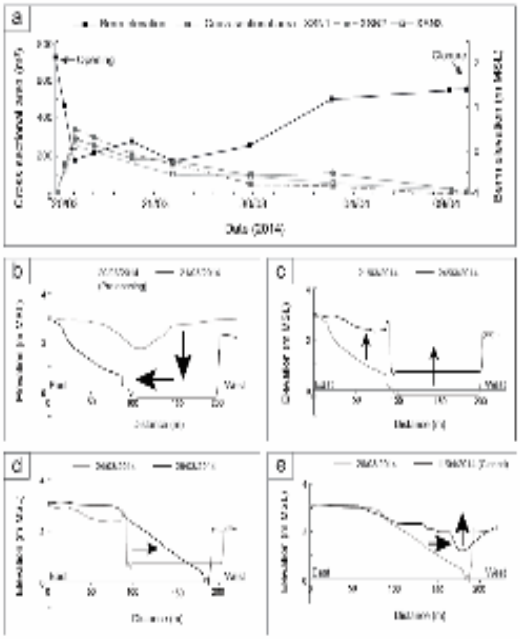

Figure 10. Change in entrance morphology at Aire River following artificial opening 1. (a) Change in berm elevation and cross sectional area from opening through to closure at all cross sections; (b) Cross section 1 (XSN1) 20/03/2014 - 21/03/2014 (pre - post-opening), incision is dominant. The arrows represent the direction of sediment movement with the size representing the magnitude of sediment movement; (c) 21/03/2014 - 24/03/2014 (small amount of lateral infill from eastern side); (d) 24/03/2014 - 26/06/2014 (further infill from east); (e) cross section 26/03/2014 - 11/04/2014 (further infill until closure).

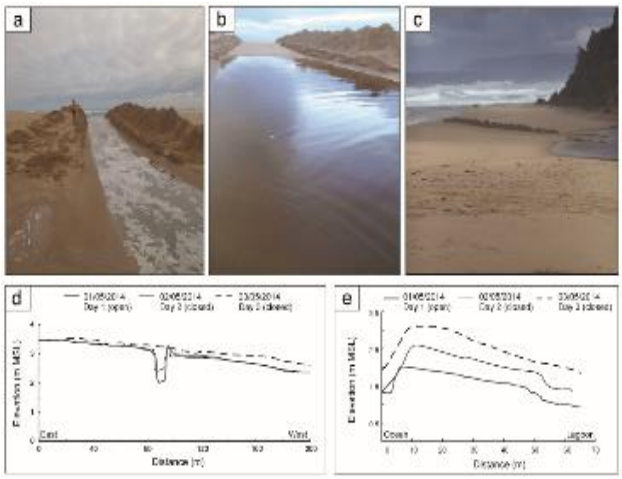

Figure 11. Change in entrance morphology at Aire River following artificial opening 2. (a) Day 1 of monitoring 01/05/2014; (b) Day 2 of monitoring (02/05/2014) - entrance closed, vertical infill of channel bed; (c) Day 3 of monitoring (03/05/2014) - closed entrance, further vertical accretion; (d) channel crosssections 01/05/2014 - 03/05/2014; (e) long profiles 01/05/2014 - 03/05/2014.

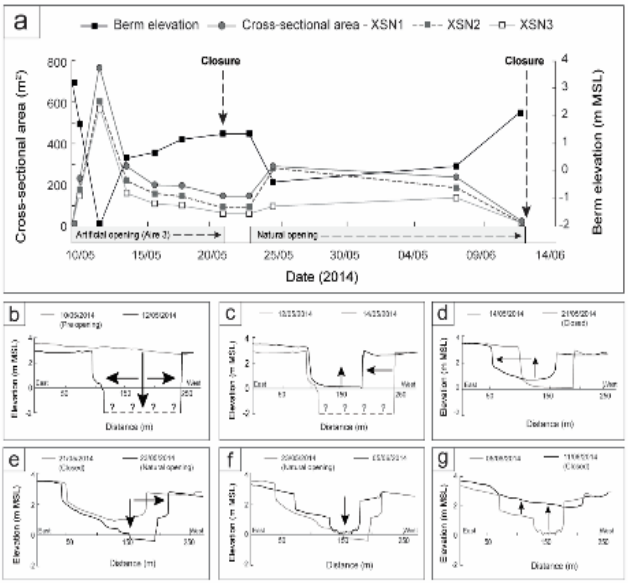

Figure 12. Change in entrance morphology at Aire River following artificial opening 3 and including a natural opening occurring on 23/05/2014. (a) Change in berm elevation and cross sectional area from opening through to closure; (b) cross section 1 (XSN1) 10/05/2014 - 12/05/2014 (pre - post-opening), incision is dominant. The arrows represent the direction of sediment movement with the size representing the magnitude of sediment movement; (c) 12/05/2014 - 14/05/2014; (d) 14/05/2014 - 21/05/2014 (entrance closure on 21/05/2014); (e) 21/05/2014 - 23/05/2014 (closure - natural opening, incision dominant); (f) 23/05/2014 - 05/06/2014 (narrowing of channel); (g) 05/06/2014 - 11/06/2014 (further infill and entrance closure).

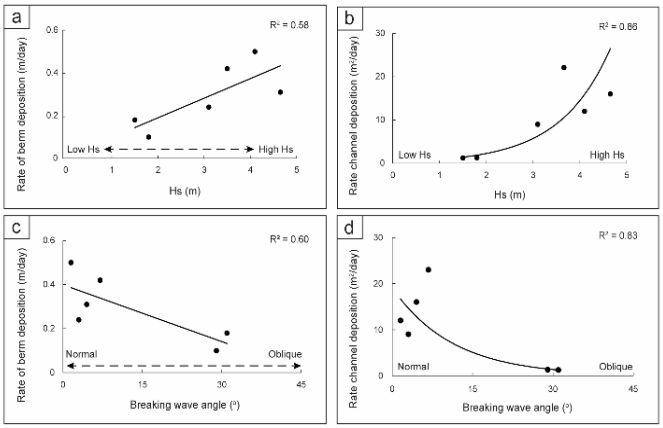

Figure 13. Rates of change in berm and channel deposition in relation to (a) (b) offshore wave height and (c) (d) wave direction (in relation to shore normal) at all entrance openings. Rate of deposition is taken from when the estuary became depositional as indicated in morphological surveys and through to the day of closure. Wave data averaged across all days the estuary was in a depositional state.

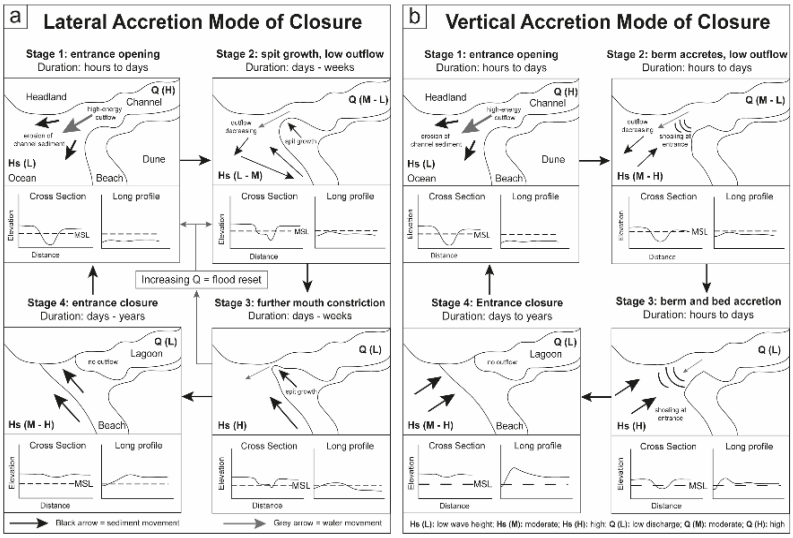

Figure 14: Modes of entrance closure as observed in IOCE in Victoria, Australia: (a) lateral accretion (b) vertical accretion. Schematic change in channel morphology is shown from an open entrance (Stage 1) through to reclosure (Stage 4). Cross sectional morphology and long profiles during each stage are also shown.